

Excitonic transitions in strained-layer $\text{In}_x\text{Ga}_{1-x}\text{As}/\text{GaAs}$ quantum wells

D. Gershoni, J. M. Vandenberg, S. N. G. Chu, H. Temkin, T. Tanbun-Ek, and R. A. Logan

AT&T Bell Laboratories, Murray Hill, New Jersey 07974

(Received 5 July 1989)

A study of the excitonic transitions in pseudomorphic quantum wells of $\text{In}_x\text{Ga}_{1-x}\text{As}$ grown on GaAs substrates is presented. The experimental data obtained by photoluminescence excitation and absorption techniques agree very well with our theoretical model. The model is based on phenomenological deformation potential theory and includes band nonparabolicity and valence-band-mixing terms. The same model, without any adjustable parameters, was also applied successfully to the $\text{In}_x\text{Ga}_{1-x}\text{As}/\text{InP}$ system before.

Strained-layer superlattices (SLS) and quantum wells (SLQW) have recently been the subject of great interest in both theory¹⁻¹⁰ and experiment.¹⁰⁻²³ Particular attention was paid to carriers' confined levels and optical transitions between them. The $\text{In}_x\text{Ga}_{1-x}\text{As}/\text{GaAs}$ material system, in particular, has been intensively studied, mainly due to its technological importance. Though numerous papers have been written on the excitonic transitions in this system, the assignment of the observed optical transitions is still debated. Many of these studies present attempts to fit the data with adjustable parameters that have no physical significance. As a result comparison with other well studied material systems cannot be done, and a better understanding of basic problems such as band alignment under lattice mismatch strain is not gained.

Here we present an experimental optical study of four very well-characterized strained-layer multi-quantum-well samples. The observed excitonic transitions are assigned using an effective mass model which takes into account both strain and nonparabolicity. For the first time no adjustable parameters are used to explain the observed transitions. The agreement with the experiment is very good. In particular, we show that for light holes the system behaves like a type-II superlattice, namely, while electron and heavy holes are confined to the strained $\text{In}_x\text{Ga}_{1-x}\text{As}$ well, light holes are weakly confined to the GaAs barriers. The model successfully assigns all the observed excitonic transitions for a wide range of strain, quantum sizes, and transition orders. This is even more convincing, since the same model and input parameters are in very good agreement with all the observed optical transitions in the $\text{In}_x\text{Ga}_{1-x}\text{As}/\text{InP}$ system as well.²¹

The $\text{In}_x\text{Ga}_{1-x}\text{As}/\text{GaAs}$ strained-layer multi-quantum-well samples were grown in an atmospheric pressure metal-organic-vapor-phase-epitaxial (MOVPE) system previously described.²⁴ They were grown on a (100)-oriented GaAs substrate followed by 0.5- μm -thick undoped GaAs buffer layer. The samples consist of 20 periods of strained $\text{In}_x\text{Ga}_{1-x}\text{As}$ quantum wells, separated by ~ 200 - \AA thick GaAs barriers. Well widths varied from ~ 50 to ~ 250 \AA in different samples. The InAs mole fraction was varied from $x=6\%$ to 24%. The growth sequence ended with the last GaAs barrier to grow.

Well dimensions and strain components parallel to the growth direction were determined by fitting the satellite pattern in the (400) high-resolution x-ray-diffraction (HRXRD) rocking curves with a kinematic step-model simulation described previously.²⁵ Dimensions and sample quality were also verified using cross-section transmission electron microscope (TEM). The agreement between both techniques was good. Thus we estimate that the maximum experimental uncertainty in the quantum-well widths is ± 6 \AA , and the InAs mole fraction is determined to within 1%. One sample (12% InAs, 245- \AA quantum well) is far over the critical layer thickness for this concentration [~ 150 \AA (Ref. 26)]. Indeed, in the TEM picture, dislocations were seen in the interface between the first quantum well and the buffer layer. No misfit dislocations are observed in the rest of the interfaces. We thus believe that the entire periodic structure maintain an equilibrium in plane lattice constant, which is slightly different from that of the GaAs. The difference is estimated from the measured density of dislocations²⁷ ($\sim 3 \times 10^4 \text{ cm}^{-1}$). Its value (0.02%) is so small, that it cannot be detected by the HRXRD measurements and it would not affect the model discussed below.

For the photoluminescence-excitation (PLE) measurements, the as-grown samples were placed in a He flow cryostat. Light from a tungsten lamp was dispersed by a 0.64-m monochromator and used as a continuously tunable source of excitation. The photoluminescence (PL) was monitored by a second 0.64-m monochromator followed by a liquid-nitrogen cooled germanium detector. The spectra were corrected later for the system response. Figure 1 presents the PLE spectra (solid lines) and PL spectra (dashed lines) of the samples. The bars indicate excitonic transition energies calculated using the model described below. The PL lines are due to the excitonic recombination of electrons and heavy holes from the $n=1$ subband levels. The lines are shifted down in energy from the same lines observed in the PLE spectra. This energy shift (also known as "Stokes shift") as well as the line narrowing of the PL spectra relative to the corresponding PLE lines, can be explained in terms of recombination processes which involve excitons bound to potential fluctuations in the ternary quantum wells. Similar behavior was observed and discussed for quantum wells of $\text{In}_x\text{Ga}_{1-x}\text{As}$ grown on InP.²⁸ Potential fluctuations

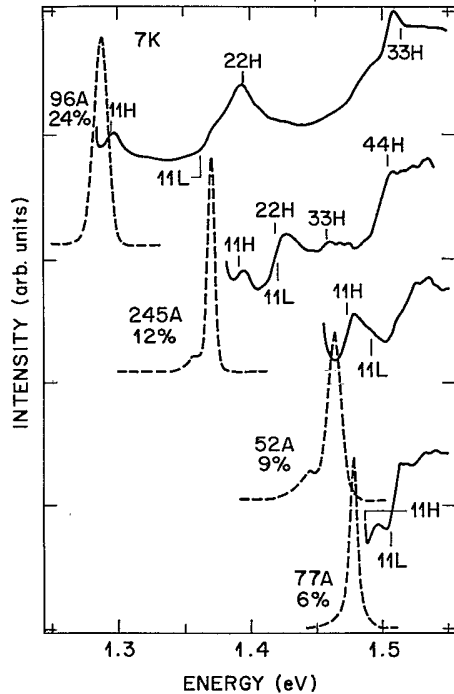


FIG. 1. Low-temperature PL (dashed lines) and PLE (solid lines) spectra of four strained-layer $\text{In}_x\text{Ga}_{1-x}\text{As}/\text{GaAs}$ multi-quantum-well samples. Vertical bars indicate calculated excitonic transitions. The first number above the bar refers to the conduction-band sublevel, the second to the valence-band sublevel, and the letter H (L) indicates that this is a heavy- (light-) hole subband.

within the ternary quantum wells contribute also to the energy width of the excitonic transitions which are observed in the PLE spectra of all the samples in Fig. 1. The excitonic features are much wider than those observed in binary quantum wells of GaAs in the GaAs/ $\text{Ga}_{1-x}\text{Al}_x\text{As}$ system.²⁹ This phenomenon of inhomogeneous line broadening is very well known in bulk ternary crystals.³⁰ It manifests itself in a similar way in ternary quantum wells as well. Since these potential fluctuations are intrinsic to $\text{In}_x\text{Ga}_{1-x}\text{As}$ quantum wells, it is difficult to saturate the luminescence from them by increasing the excitation density. Indeed the PL line energies were found to be independent of excitation density up to $\sim 10 \text{ kW/cm}^2$. This, however, cannot be used as an indication that the PL lines originate from free exciton recombination.²³ At very low excitation densities additional lower-energy lines in the PL spectra are observed (Fig. 1, 9% and 12% samples). We attribute these lines to excitonic recombination associated with extrinsic defects in the material. The lines saturate easily with increasing excitation density.

Another dissimilarity between this material system and the GaAs/ $\text{Ga}_{1-x}\text{Al}_x\text{As}$ one, is the absence of light holes to electron excitonic transitions, as can be seen in Fig. 1. In the following we argue that this is due to the strain induced energy bands alignment which is unique to this system. As a result, light holes are confined in the GaAs barriers so that the spatial overlap between their wave functions and the electrons' wave functions are small. The cal-

culated energies for these $n=1$ spatially indirect transitions are also marked in Fig. 1 by vertical bars below the PLE curves. Note that only one spectral feature, namely the shoulder below the 22H transition of the $x=24\%$ sample can be explained this way.

The theoretical model, which assigns the observed transitions in Fig. 1, was used by us before to assign the observed transitions in strained-layer quantum wells of $\text{In}_x\text{Ga}_{1-x}\text{As}$ grown on InP.²¹ Thus, we only briefly review it here.

Commensurate growth of strained $\text{In}_x\text{Ga}_{1-x}\text{As}$ layers on (100)-oriented GaAs substrate results in a biaxial compressive strain in the layer plane. The only nonvanishing components of the strain tensor are the diagonal ones. They obey the following relations:

$$\epsilon_{xx} = \epsilon_{yy} = \epsilon_{\parallel}, \quad (1a)$$

$$\epsilon_{zz} = -[2C_{12}(x)/C_{11}(x)]\epsilon_{\parallel} = \epsilon_{\perp}, \quad (1b)$$

$$\epsilon_{\parallel} = [a_{\text{GaAs}} - a(x)]/a(x), \quad (1c)$$

$$\epsilon_{\perp} = a_{\perp}/a(x). \quad (1d)$$

In Eqs. (1), \hat{z} was chosen along the growth direction, C_{ij} are the components of the elastic stiffness tensor, a_{GaAs} is the GaAs lattice constant and $a(x)$ is the unstrained lattice constant of the ternary $\text{In}_x\text{Ga}_{1-x}\text{As}$. a_{\perp} is the layer lattice constant in the growth direction.

Since a_{\perp} can be determined directly from the HRXRD measurement, Eq. (1) is used to determine the exact composition (x) and the strain in the $\text{In}_x\text{Ga}_{1-x}\text{As}$ quantum-well layer. In doing so we use linear interpolation between the known values of the binary parents' stiffness tensor components and lattice constants, to obtain those of the ternary. Band gaps of the relaxed $\text{In}_x\text{Ga}_{1-x}\text{As}$ are calculated using a parabolic interpolation between the known band gaps of InAs, GaAs, and $\text{In}_{0.53}\text{Ga}_{0.47}\text{As}$ lattice matched to InP. Valence-band offsets between relaxed $\text{In}_x\text{Ga}_{1-x}\text{As}$ and GaAs are calculated using a linear interpolation between 0 (GaAs/GaAs) and 0.07 eV (InAs/GaAs). The last point is taken from a recent compilation of experimental x-ray photoemission spectroscopy (XPS) data.³¹ Though the uncertainty in this value is quite large (~ 0.1 eV), no better determination is available. This procedure that we have first suggested to use for the $\text{In}_x\text{Ga}_{1-x}\text{As}/\text{InP}$ system¹³ is now shown to be valid.^{16,18} It also gains support from the more recent model-solid theory.³ Finally, band gaps, hydrostatic, and shear deformation potentials are linearly interpolated from those of the binary parents and strain-induced corrections to the ternary band-edge energies are calculated using phenomenological deformation potential theory [Eqs. (2)–(4) of Ref. 21].

In Fig. 2 we display the calculated band-edge energies for strained $\text{In}_x\text{Ga}_{1-x}\text{As}$ relative to the valence band of the GaAs substrate. For comparison with the experiment, the observed lowest optical transitions, corrected for the quantum size effect, are also shown (solid arrows). As can be seen in the figure, for the $x < 0.6$ region, the light-hole valence band of the strained $\text{In}_x\text{Ga}_{1-x}\text{As}$ layer falls

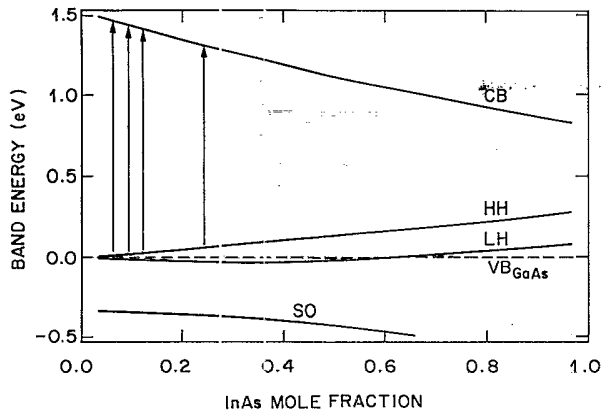


FIG. 2. Calculated band energies for strained layers of $\text{In}_x\text{Ga}_{1-x}\text{As}$ grown on (100) GaAs as a function of x . Energy is measured relative to the GaAs valence band. Measured optical transitions, corrected for the quantum size effect are shown (vertical arrows) for comparison.

below the GaAs degenerate valence band. Thus for light holes the system behaves like a type-II superlattice. This is in agreement with previous works,^{11,20} but in clear contradiction with the conclusions of Menendez *et al.*¹⁹ It is also important to point out that the observed excitonic transitions cannot be successfully fitted using a constant band offset ratio. Such fits, which have no physical justification, were attempted in the past by a few groups.^{15,17,20} It is clear from Fig. 2 that such a ratio (usually defined as $Q_c = \Delta E_c / \Delta E_g$) must be composition (x) dependent. As such it does not contribute anything to our understanding. Heterostructure systems are characterized well by the valence-band offset. For III-V ternary alloys the last seems to follow linear dependence on composition.^{16,18,21} Since the band gap of those ternaries is known to follow nonlinear dependence on the composition (bowing), there is no reason whatsoever to expect that the band offset ratio (Q_c) will be composition independent.

For the sake of comparison between our work and previous fits we note that for small enough InAs mole fraction ($x < 0.15$) one can approximate both the heavy-hole valence band and the conduction band as linearly dependent on x . For this case we found that $Q_c(x < 0.15) = 0.77$. This value agrees with few previous fits^{15,20,23} but disagrees with Ref. 19.

In order to calculate the carriers' subband energies due to the quantum size effect, we have solved numerically the finite quantum-well problem for each carrier separately, using band edges from Fig. 2. Zone center masses are linearly interpolated from the binary values (all input parameters are listed and referenced in Table I of Ref. 21), and strain corrections to light holes due to mixing with the split-off band are introduced.³² Band nonparabolicity is taken into account through the energy dependence of the effective mass. This dependency, in turn, is given implicitly by the Kane model dispersion relations, which we apply to the corrected band edges.²¹ Finally, the exciton binding energy is calculated using a two-dimensional hydrogenlike model. This term is usually less than the experi-

mental linewidth, so that a more delicate treatment is unnecessary.

As can be seen in Fig. 1, our model gives good assignments to all the observed excitonic resonances to allowed heavy-hole electron transitions. One spectral feature, namely the shoulder below the 22H transition of the $x = 24\%$ sample is energetically assigned to the GaAs light hole, $\text{In}_x\text{Ga}_{1-x}\text{As}$ electron transition. Similar features have been reported also by others.^{11,23} We used our model to calculate the overlap integral between the two spatially separated wave functions. Due to the small potential step and the small mass of the light hole, it is indeed only slightly confined within the barriers, and the overlap amounts to $\sim 20\%$. Thus, the optical transition is not forbidden but one should not expect excitonic resonance, similar in appearance to transitions associated with heavy holes.

Finally, in order to confirm our assignments, we have measured the room-temperature polarized transmission and photocurrent spectra of all the samples. Polarized light was launched into cleaved facet of 2-mm-long sample by a $\times 50$ microscope objective and was gathered in the same way from the other cleaved side. In order to avoid waveguiding effects which favor transmission of light polarized parallel to the growth direction (TM), the transmission is normalized to 100% at some low energy, below the last exciton transition. (The photocurrent spectra were also obtained under the same conditions.) In Fig. 3 we display both the photocurrent and transmission spectra of the $x = 24\%$ sample. The TE polarized spectrum is represented by a solid line and the TM by a dashed line. The three excitonic transitions which are observed in the low-temperature PLE spectra are also observed here. The absorption which is preferably polarized in the quantum-well plane (TE), confirms that the transitions are associated with heavy-hole states.³³

In summary, we present a study of excitonic transitions in pseudomorphic quantum wells of $\text{In}_x\text{Ga}_{1-x}\text{As}/\text{GaAs}$.

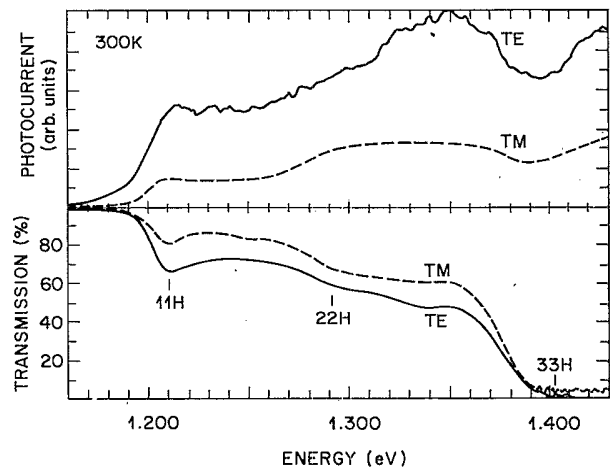


FIG. 3. Room-temperature polarized transmission and photocurrent spectra of the $x = 24\%$ sample. Solid (dashed) lines represent light polarized perpendicular (parallel) to the direction of growth—TE (TM). Vertical bars indicate excitonic transitions.

We have investigated a set of very well-characterized samples, chosen to cover a wide range of biaxial strain. Experimental exciton energies are compared with a model based on phenomenological deformation potential and elastic theories. The model which includes nonlinear terms in strain and band nonparabolicity, accounts very

well for all the observed transitions. The same model with the same input parameters, none of them adjustable, also explains all the observed transitions in quantum wells of strained $\text{In}_x\text{Ga}_{1-x}\text{As}$ grown on InP. In particular, we have established that for $x < 0.25$ light holes are weakly confined within the GaAs barriers.

- ¹G. C. Osbourn, *Phys. Rev. B* **27**, 5126 (1983).
- ²M. Cardona and N. E. Christensen, *Phys. Rev. B* **35**, 6182 (1987).
- ³C. G. Van De Walle, *Phys. Rev. B* **39**, 1871 (1989).
- ⁴S. Froyen, D. M. Wood, and A. Zunger, *Phys. Rev. B* **37**, 6893 (1988).
- ⁵R. People, *IEEE J. Quantum Electron.* **QE-22**, 1696 (1986).
- ⁶M. S. Hybertsen and M. Schluter, *Phys. Rev. B* **36**, 9683 (1987).
- ⁷G. D. Sanders and K. K. Bajaj, *Phys. Rev. B* **35**, 2308 (1987).
- ⁸G. Platero and M. Altarelli, *Phys. Rev. B* **36**, 6591 (1987).
- ⁹L. C. Andreani, A. Pasquarello, and F. Bassani, *Phys. Rev. B* **36**, 5887 (1987).
- ¹⁰S. C. Hong, G. P. Kothiyal, N. Debbar, P. Bhattacharya, and J. Singh, *Phys. Rev. B* **37**, 878 (1988).
- ¹¹J. Y. Marzin, M. N. Charasse, and B. Sermage, *Phys. Rev. B* **31**, 8298 (1985).
- ¹²I. J. Fritz, L. R. Dawson, J. J. Drummond, J. E. Schirber, and R. M. Biefeld, *Appl. Phys. Lett.* **48**, 139 (1986).
- ¹³D. Gershoni, J. M. Vandenberg, R. A. Hamm, H. Temkin, and M. B. Panish, *Phys. Rev. B* **36**, 1320 (1987).
- ¹⁴C. P. Kuo, S. K. Vong, R. M. Cohen, and G. B. Stringfellow, *J. Appl. Phys.* **57**, 5428 (1985).
- ¹⁵T. G. Anderson, Z. G. Chen, V. D. Kulakovskii, A. Uddin, and J. T. Vallin, *Phys. Rev. B* **37**, 4032 (1988).
- ¹⁶D. Gershoni, H. Temkin, J. M. Vandenberg, S. N. G. Chu, R. A. Hamm, and M. B. Panish, *Phys. Rev. Lett.* **60**, 448 (1988).
- ¹⁷U. Cebulla, G. Trankle, U. Zien, A. Forchel, G. Griffiths, H. Kroemer, and S. Subbana, *Phys. Rev. B* **37**, 6278 (1988).
- ¹⁸R. E. Cavicchi, D. V. Lang, D. Gershoni, A. M. Sergant, J. M. Vandenberg, S. N. G. Chu, and M. B. Panish, *Appl. Phys. Lett.* **54**, 739 (1989).
- ¹⁹J. Menendez, A. Pinczuk, D. J. Werder, S. K. Sputz, R. C. Miller, D. L. Sivco, and Y. Cho, *Phys. Rev. B* **36**, 8165 (1987).
- ²⁰G. Ji, D. Huang, U. K. Reddy, T. S. Henderson, R. Houdre, and H. Morkoc, *J. Appl. Phys.* **62**, 3366 (1987).
- ²¹D. Gershoni, H. Temkin, M. B. Panish, and R. A. Hamm, *Phys. Rev. B* **39**, 5531 (1989).
- ²²M. J. Joyce, M. J. Johnson, M. Gal, and B. F. Usher, *Phys. Rev. B* **38**, 10978 (1988).
- ²³K. F. Huang, K. Tai, S. N. G. Chu, and A. Y. Cho, *Appl. Phys. Lett.* **54**, 2026 (1989).
- ²⁴R. A. Logan, T. Tanbun-Ek, and A. M. Sergant, *J. Appl. Phys.* **65**, 3723 (1989).
- ²⁵J. M. Vandenberg, S. N. G. Chu, R. A. Hamm, M. B. Panish, and H. Temkin, *Appl. Phys. Lett.* **49**, 1302 (1986).
- ²⁶J. W. Matthews and A. E. Blakeslee, *J. Cryst. Growth* **27**, 118 (1974).
- ²⁷S. N. G. Chu, A. T. Macrander, K. E. Sterge, and W. D. Johnston, Jr., *J. Appl. Phys.* **57**, 249 (1985); **60**, 1238 (1986).
- ²⁸D. Gershoni, H. Temkin, and M. B. Panish, *Phys. Rev. B* **38**, 7870 (1988).
- ²⁹See, for example, R. C. Miller, D. A. Kleinman, W. A. Nordland, Jr., and A. C. Gossard, *Phys. Rev. B* **22**, 863 (1980).
- ³⁰See, for example, *Excitons*, edited by E. I. Rashba and M. D. Sturge (North-Holland, Amsterdam, 1982).
- ³¹R. S. Bauer and G. Margaritondo, *Phys. Today* **40**, No. 1, 27 (1987), and references therein.
- ³²H. Hasegawa, *Phys. Rev.* **129**, 1029 (1963).
- ³³J. C. Hensel and G. Feher, *Phys. Rev.* **129**, 1401 (1963); J. S. Weiner, D. S. Chemla, and D. A. B. Miller, *Appl. Phys. Lett.* **47**, 664 (1985).